

Formation or cleavage of rings via sulfide-mediated reduction offers background-free detection of sulfide

Sanjib Ghosh, Biswajit Roy, and Subhajit Bandyopadhyay

J. Org. Chem., **Just Accepted Manuscript** • DOI: 10.1021/acs.joc.9b01946 • Publication Date (Web): 28 Aug 2019

Downloaded from pubs.acs.org on August 28, 2019

Just Accepted

“Just Accepted” manuscripts have been peer-reviewed and accepted for publication. They are posted online prior to technical editing, formatting for publication and author proofing. The American Chemical Society provides “Just Accepted” as a service to the research community to expedite the dissemination of scientific material as soon as possible after acceptance. “Just Accepted” manuscripts appear in full in PDF format accompanied by an HTML abstract. “Just Accepted” manuscripts have been fully peer reviewed, but should not be considered the official version of record. They are citable by the Digital Object Identifier (DOI®). “Just Accepted” is an optional service offered to authors. Therefore, the “Just Accepted” Web site may not include all articles that will be published in the journal. After a manuscript is technically edited and formatted, it will be removed from the “Just Accepted” Web site and published as an ASAP article. Note that technical editing may introduce minor changes to the manuscript text and/or graphics which could affect content, and all legal disclaimers and ethical guidelines that apply to the journal pertain. ACS cannot be held responsible for errors or consequences arising from the use of information contained in these “Just Accepted” manuscripts.

Formation or cleavage of rings *via* sulfide-mediated reduction offers background-free detection of sulfide

Sanjib Ghosh^a, Biswajit Roy^a, Subhajit Bandyopadhyay^{*a}

^aDepartment of Chemical Sciences, Indian Institute of Science Education and Research (IISER) Kolkata, Mohanpur, Nadia 741246, India

ABSTRACT: A set of three highly selective probes for sulfide detection has been developed. Two novel mechanistic strategies for the detection, including (a) transformation of a pro-fluorophore into an active fluorophore, and (b) destruction of a fused ring to activate a fluorophore, have been explored. The structural features of the probes including azido groups ('active' and 'latent') and leaving groups (with or without attached to the fluorophore) have been investigated. During the course of the mechanistic studies, the single crystal structures of all the probes and the products were obtained. One of the probes proved to be superior in terms of its ability to detect sulfide in pure water *via* an *in situ* formation of a fluorophore from a non-fluorescent precursor. These cheap and easy-to-prepare probes offer practical applications of sulfide recognition in environmental water samples and in the ovaries of fruit-flies. A detection and quantification method using one of these probes and analysis with a smartphone enabled non-specialists to detect sulfide reliably.

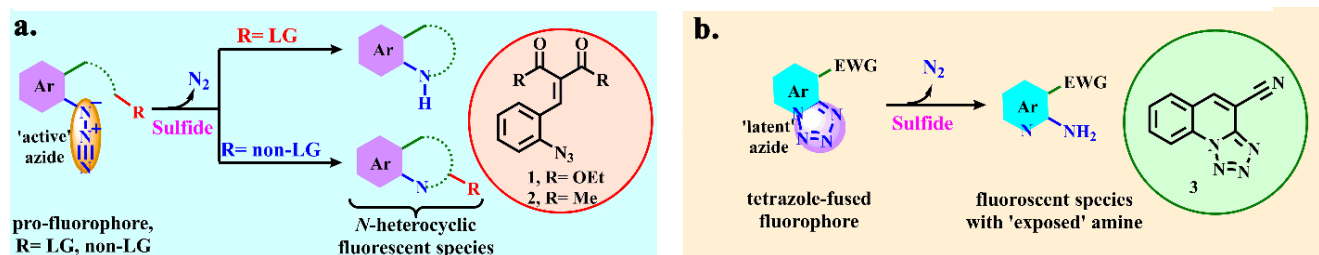
INTRODUCTION

Hydrogen sulfide has a significant physiological and pathological role in biological systems.¹⁻⁴ Nevertheless, H₂S is a hazardous sewer gas which is largely produced by industrial processes and organic wastes that pollutes the water-bodies. Its toxic effects depend on its concentration and the exposure time. Exposure to sulfide concentrations in the range of 10-500 ppm, may result in rhinitis and acute respiratory paralysis.⁵ However, under a long-term exposure or higher concentration only a few breaths are required to cause coma, brain damage, and death.⁶⁻⁷ As the 'knock down gas', it has caused many such mishaps of occupational toxic exposure where mining labourers have been knocked unconscious and killed.⁸ H₂S, similar in

toxicity with HCN and CO, has resulted in mass destruction through accidental leakage.⁹⁻¹¹ It has also been used as a chemical weapon.¹² Alarmingly, it has become a popular tool for committing chemical suicide as well as in the attempt of orchestrating terror plots.¹³⁻¹⁵ While it influences the proliferation of cancer cell,¹⁶ altered levels of H₂S have been linked to Alzheimer's disease,¹⁷ Down's syndrome,¹⁸ diabetes¹⁹ and liver cirrhosis.²⁰

H₂S is a silent killer. Though sulfide has a characteristic malodor, it is not a reliable indicator. While exposure to high level (>150 ppm) of sulfide numbs the smelling sensation instantly, the minimum perceptible odor of H₂S is reported to be 0.13 ppm.²¹ The underlying toxicological mechanism is yet to be explored in detail and sulfide poi-

Scheme 1. Schematic representation of the strategies adopted in this work^{a,b}



^aTransformation of a pro-fluorophore into another fluorescent species *via* cyclization and ^bdestruction of the ring fused with the fluorophore where LG and EWG refer to 'Leaving Group' and 'Electron-withdrawing Group' respectively; (inset) structures of probes **1**, **2** and **3** are shown in circles.

soning lacks specific therapy.²² Therefore, a fast and precise method for the detection of sulfide is of utmost importance.

The importance and applications of fluorimetric method of sulfide detection has been reiterated in the literature.^{23–29} The principal detection strategies include metal precipitation, nucleophilic attack, and reduction of azide (or nitro) groups. A popular strategy is the sulfide-induced reduction of an azido group, directly^{30–35} (or indirectly, through a spacer^{36–40}) attached to a fluorophore, into an amine which turns on the fluorescence generally through a charge transfer (Scheme S1). In 2011, Chang has been the pioneer to introduce the azide-based sulfide probes.⁴¹ Since then, more than 100 papers have been published underlining the dominance of this detection strategy (see Supporting Information for references). However, over-exploitation of this method with mere change in the fluorophore led to the loss of its novelty and academic interest. Therefore, this vastly used method warrants improvisation and added features to broaden the scopes and improve on the detection.

This work explores the detection of sulfides *via* two novel strategies. The first one deals with a sulfide-mediated reduction of an azide and a subsequent annulation, forming a new fused-ring system. The second strategy exploits a non-fluorescent tetrazine ring system that can be formally considered as a “latent (or camouflaged) azide”. Reduction of the latent azide destroys the fused ring, ensuing a push-pull mechanism.

We envisaged that each of the pro-fluorophores can undergo transformation from an open chain aryl derivative (or a fused ring system) to an *N*-heterocyclic fluorescent species with better delocalization (and perhaps greater structural rigidity) and consequently a red-shifted emission maximum (Scheme 1). The open chain could be flanked by a leaving or a non-leaving group. Probes **1** and **2** were thought to be an ideal manifestation of these ideas respectively (Scheme 1a). On the other hand, the azide group might also remain ‘latent’ as a tetrazole ring, fused with a fluorophore that may undergo the removal of the ring to revive the actual emission of the fluorophore. Probe **3** could be proved to be a perfect candidate, befitting this scheme (Scheme 1b).

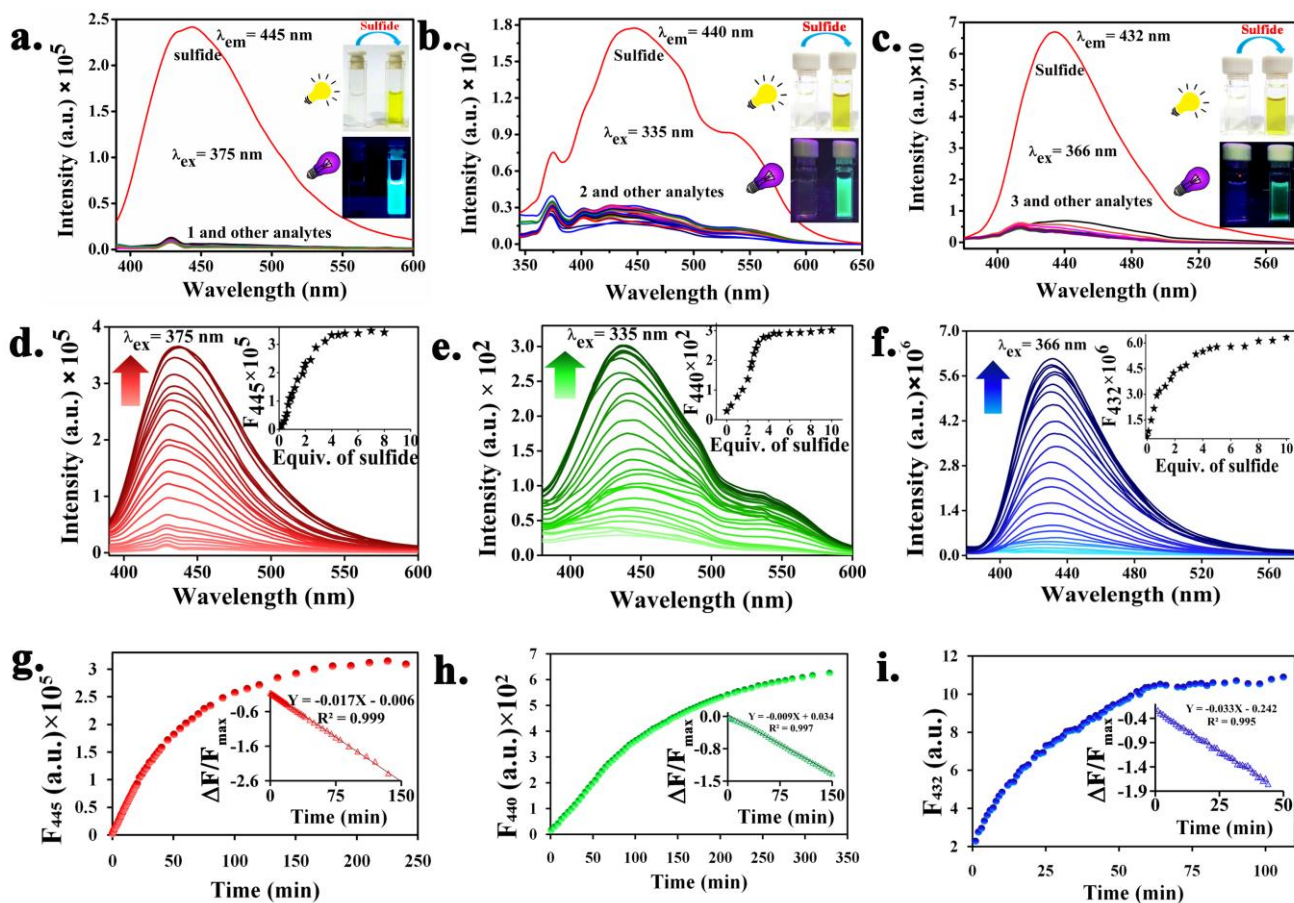


Figure 1. Fluorescence spectral changes of (a) probe **1**, (b) probe **2** and (c) probe **3** (100 μ M each) upon addition of various analytes (0.6 mM each); (inset) visual changes of the respective probes before and after addition of sulfide under ambient light (above) and UV light (below). Fluorescence enhancement of (d) probe **1** (e) probe **2** and (f) probe **3** (100 μ M each) along with the titration profile of each probe (shown in inset) upon addition of sulfide. Time-dependent studies of (g) probe **1**, (h) probe **2** and (i) probe **3** (100 μ M each) in the presence of sulfide (400 μ M); (inset) kinetic profiles for the sulfide-induced reaction undergone by the respective probes.

RESULTS AND DISCUSSION

Experiments were performed in milli-Q water (for probe 1) and water-acetonitrile mixture (for probes 2 and 3) at pH 7.4 at 25 °C with 100 μM probe in each case unless otherwise indicated. The 'addition of sulfide' is simply to be understood as 'addition of Na₂S' unless otherwise indicated.⁴² The preliminary spectroscopic analyses caused the emission bands of the probes 1, 2 and 3 to shift from 430 to 445 nm ($\lambda_{\text{ex}} = 375$ nm), 425 to 440 nm ($\lambda_{\text{ex}} = 335$ nm), and 414 to 432 nm ($\lambda_{\text{ex}} = 366$ nm), respectively, with a dramatic emission enhancement in the presence of Na₂S (6 equiv.) in each case (Figure 1a–c). In contrast, the fluorescence profile seemed to remain practically unaffected in the presence of other anions and small molecules suggesting the specific nature of the probes toward sulfide.

Probe 1 displayed discrete absorption bands at 250, 286 and 335 nm. Addition of sulfide (0–6 equiv.) to probe 1 exhibited a decrease in absorbance at λ_{abs} 286 nm with a small blue shift for all the bands. While probe 2 showed a gradual decrease in the absorbance at 280 and 330 nm, probe 3 exhibited increments at 300 and 330 nm. All these changes are in conformity with the predicted spectra of the desired species (Figure S1). The probe 1 ($\Phi = 0.004$), 2 ($\Phi = 0.0003$), and 3 ($\Phi = 0.002$) (with respect to quinone sulfate) brought about small red shifts (~15 nm for each of the probes) in the emission maximum along with significant enhancement i.e. 70-fold for probe 1, 10-fold for probe 2 and 70-fold for probe 3 (with Φ being 0.015, 0.006 and 0.006 respective-

ly), at λ_{em} 445, 440 and 432 nm respectively, linearly varying with the concentration of sulfide from 0 to 4 equiv. (Figure 1d–f, Supporting Information). The limits of detection (LOD) were found to be 2.07, 0.67 and 1.73 μM for probes 1, 2 and 3, respectively (Figure S2, Supporting Information).⁴³

The time-dependent emission studies of the sulfide-induced reaction of probes 1, 2 and 3 showed that the progress of the reaction reached a plateau after 180, 300 and 60 min, respectively, and followed a pseudo-first order kinetics with rate constants of 0.017, 0.0091, and 0.033 min⁻¹ respectively (Figure 1g–i). Visibly, the changes in fluorescence intensity could be observed within 30 minutes after the addition of the sulfides to the probes as the emission intensity reached 43%, 25% and 70% of the respective saturation point with the probes 1, 2 and 3, respectively. Of course, the time to reach the saturation fluorescence intensity took longer. Competitive experiments with various biologically and environmentally relevant analytes including oxidants (e.g. H₂O₂, perborate, aerial oxygen.) reductants (e.g. ascorbate, S₂O₃²⁻, S₂O₄²⁻, S₂O₅²⁻), and nucleophiles (e.g. HSO₃⁻, CN⁻, SCN⁻), displayed no significant disruption of the sulfide-induced fluorescence response (Figure S3). The pH variation studies on the fluorescence response of the probes showed steady responses over a broad pH range (3.0–9.0) in the presence of sulfide, adding to the compatibility of the probe under different conditions (Figure S4). The reaction mixtures of each of 1, 2 and 3 with sulfide were monitored

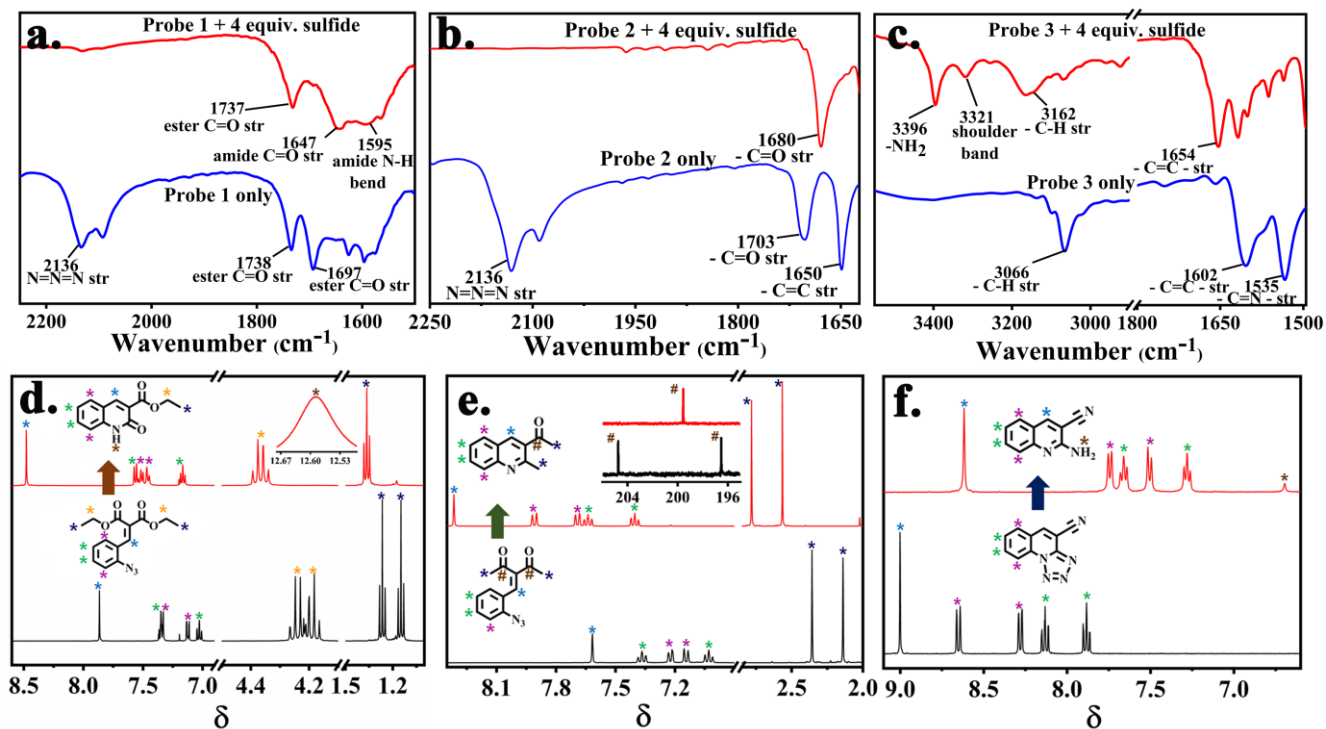


Figure 2. Comparative FT-IR (partial) spectra of (a) probe 1, (b) probe 2 and (c) probe 3 in the presence and the absence of sulfide. Comparative ¹H NMR (partial) spectra of (d) probe 1 in CDCl₃ (inset: the peak for –CONH proton), (e) probe 2 in CDCl₃ (inset: comparative ¹³C NMR (partial) spectra before and after addition sulfide) and (f) probe 3 in DMSO-*d*₆/CD₃CN (2:1; v/v) in the presence and the absence of sulfide.

by TLC.

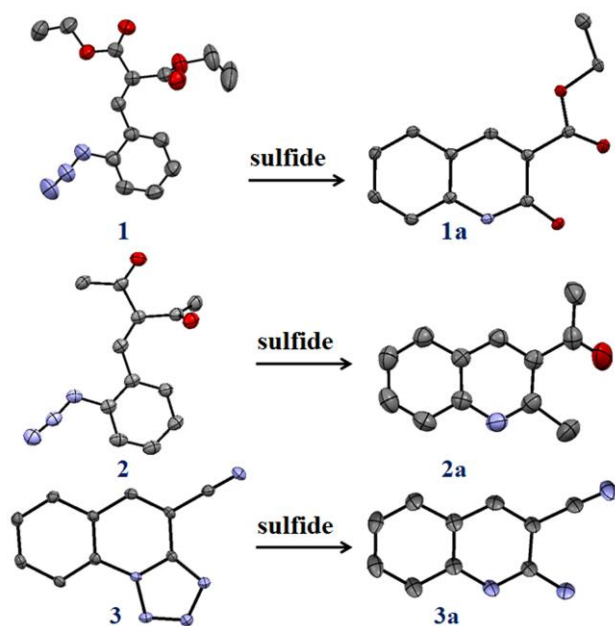


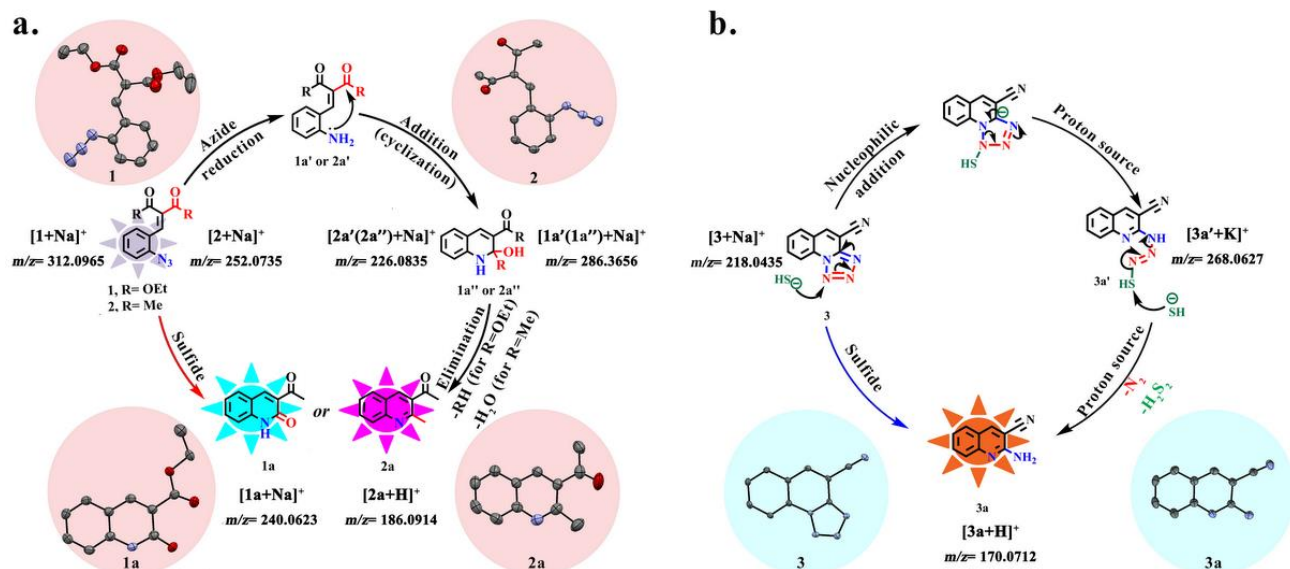
Figure 3. Crystal structures of the probes and their corresponding products obtained upon addition of sulfide. All the structures are associated with thermal ellipsoid plot with 50% probability; All the structures are with 50% Hydrogens are omitted for clarity.

A newly generated polar, fluorescent component was seen to exist on the TLC plate for each of the probes upon treatment with sulfide. FTIR spectra after the addition of sulfide displayed new bands with distinct changes. (Figure 2a–c, S5). The disappearance of the azido ($-N_3$)

stretching frequency of probe **1** suggested a chemical transformation of the group in the presence of sulfide. For probe **1**, while one of the two ester carbonyls ($-\text{CO}_2\text{Et}$) remained intact, the other one vanished, generating new merged peaks, presumably corresponding to the $-\text{C}=\text{O}$ stretching and the amide $-\text{NH}$ bending, respectively (Figure 2a, S5A). Probe **2** also showed the disappearance of azido stretching with a shift in the $-\text{C}=\text{O}$ stretching (Figure 2b, S5B). Probe **3** displayed a concomitant appearance of an $-\text{NH}$ stretching (with a characteristic shoulder band) and disappearance of the $-\text{C}=\text{N}$ stretching (of tetrazole) (Figure 2c, S5C). The ESI-MS of probes **1**, **2** and **3** after the addition of Na_2S played a crucial role in unravelling the mechanisms of detection by displaying the expected peaks for the intermediates, **1a'**, **2a'** and **3a'** for probes **1**, **2** and **3**, respectively (Scheme 2, Figure S6–8).

To obtain further insights into the mechanism of sulfide detection, time-dependent ^1H NMR titration of probe **1** was also performed (Figure S9). The titration showed that the peaks at δ 4.34 and 1.38 corresponding to the H_b and H_a gradually disappeared. Apart from other minor shifts, H_c protons went through a shift from 4.32 to 3.58. The probe **1** displayed a new broad signal appeared at δ 8.27 for the H_f which gradually broadened further and eventually vanished perhaps due to the proton exchange with the solvent. The investigation into the mechanistic detection through ^1H NMR studies continued for all the probes in order to establish the structures of the products upon addition of the sulfide and to study the mechanism in further details. (Figure 2d–f). As can be clearly seen, upon reacting with sulfide, all the ^1H peaks of the probes **1** (CDCl_3 , 10 mM) and **2** (CDCl_3 , 10 mM) underwent downfield shifts. However, the ^1H resonances underwent up-

Scheme 2. Proposed reaction mechanisms^{a,b}



Reaction mechanisms are shown for ^aprobes **1** and **2**, and ^bprobe **3** with sulfide (inset: crystal structures of the probes and the respective products). The probable intermediates are detected by mass spectrometry in support of the mechanism.

field shifts for the probe **3** (DMSO- d_6 /CD $_3$ CN (2:1; v/v), 10 mM). The addition of sulfide to probe **1** induced the generation of the least shielded broad signal appeared for the –CONH proton along with a concomitant disappearance of the peaks corresponding to one of the –COOEt groups (Figure 2d). While probe **2** displayed a downfield shift of the proton resonances along with the disappearance of one of the 13 C resonances of the two carbonyl carbons (Figure 2e), probe **3** showed an upfield shift with generation of a broad peak for –NH $_2$ (Figure 2f), providing us with a clear picture of the associated chemical changes. All these NMR spectral studies suggested clues as to the chemical transformation involved with probes in the presence of sulfide.

In the meantime, with constant efforts, the probes and the products of all these transformations were isolated from the reaction mixture with column chromatography (Experimental Section) and crystallized. The crystal structures unambiguously revealed that compounds **1a**, **2a** and **3a** contained a carboxylate, an acetyl and a cyano group, each appended to an aromatic quinoline (or quinolone) system (Figure 3). Moreover, it was found that sulfide caused compounds **2a** and **3a** to undergo ring annulation and ring opening respectively to possess transformed groups, i.e. a –CH $_3$ and an –NH $_2$ groups, respectively. All these chemical structures were in conformity with the FTIR, ESI-MS, and NMR analyses (Figure 2, Scheme 2, Supporting Information).

The spectroscopic and X-ray evidences provided us with the mechanistic insights into the sulfide-induced formation of **1a**, **2a** and **3a** from their respective precursors (Scheme 2). The presence of the ester and the acetyl groups in the close vicinity of the primary amino group generated by the *in situ* reduction of the azido group might be the main driving forces for the probes **1** and **2**,

respectively (Scheme 2a). Taking cue from the previous reports,⁴⁴⁻⁴⁵ probe **3** is envisaged to follow the mechanism proposed in Scheme 2b because of the presence of the electrophilic tetrazole moiety fused to the quinoline system which underwent ring destruction (through nucleophilic attack by sulfide) and generated the (reduced) –NH $_2$ group. While all the three probes supposedly generate N $_2$ during the reduction of the azido groups, the nucleophilic attacks and the subsequent departure of EtOH and H $_2$ O from the probes **1** and **2**, respectively, led to their corresponding products **1a** and **2a**. Interestingly, in the process of sulfide-induced reduction, the ‘latent’ azido group (of probe **3**) can be considered as a ‘caged-azide’ that undergoes a ring-opening reaction unlike the ‘free’ azido group (of probes **1** and **2**) having a linear geometry. For probes **1** and **2**, the ring formation reaction takes place after the reduction of the azide group, whereas for probe **3**, the ring destruction occurs due the reduction of the latent azide group.

The structures of all the three pairs of probes and the products were optimized (Figure S10) and the HOMO–LUMO energy differences were found to be roughly similar. (Figure S11–13). Expectedly, the daughter products, **1a**, **2a** and **3a**, were found to be associated with increasing ICT characteristics, as evident from their electronic distribution. The calculated absorption peaks were also found to be in good agreement with the experimentally observed absorption bands (Figure S14).

In a turn-on fluorescence response, a lumophore, which is generated *in situ* by the interaction between the probe and the analyte, supposedly offers no background for *in vitro* as well as *in vivo* studies, and adds a special significance to practical applications. It is important to note that the precursor **1** does not possess a potent fluorophore whereas upon its transformation to **1a** in the

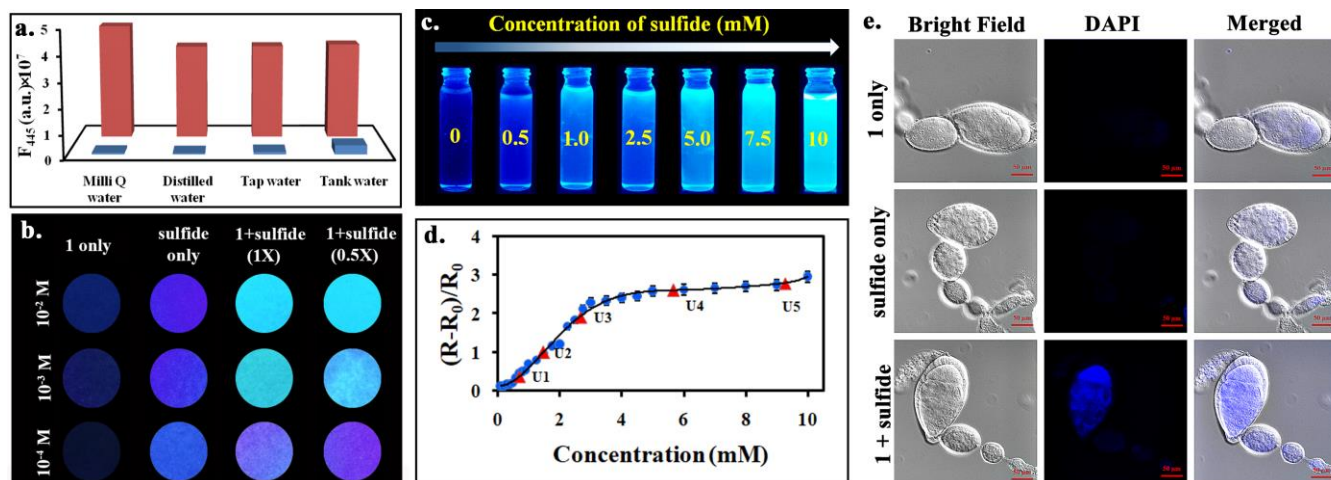


Figure 4. Fluorescence detection of sulfide with probe **1** (a) in water samples of varying contamination (showing emission response of the probe before (blue bar) and after (red bar) addition of sulfide), (b) in solution (with varying probe- and sulfide-concentration) using paper-strips, (c) with visual changes of solution under 366 nm light with a varying sulfide concentration, (d) with RGB values using calibration curve (with five blind sulfide concentrations, namely U $_1$, U $_2$, U $_3$, U $_4$ and U $_5$, marked in red triangles) and (e) in the ovary of *Drosophila* in the presence and the absence of sulfide (0.1 mM).

presence of sulfide with the additional ring fusion, a fluorescent species is generated. Since the manifestation of the fluorescence occurs only in the presence of sulfide, the chances of false positives with these probes are insignificant. Also the solubility of probe **1** is highest among the three probes of this report. In view of these special features, for practical applications for the detection of sulfides, probe **1** was chosen as a potential candidate based on its fluorescence response in aqueous medium.

Industrial effluents often pollute the aquatic environment with its sulfide content. Our probe was also applied for the detection of sulfide in water samples of varying degrees of contamination (Figure 4a) only to find that the efficiency of sulfide detection was comparable in Milli-Q, distilled, tap and tank water samples. An instrument-free dip-stick method for the qualitative detection of sulfide was also performed with this probe. Pieces of filter paper (Whatman 1, 5.5 cm × 1 cm) coated with a solution of probe **1** (10, 1 and 0.1 mM) were air-dried. The dried strips show a negligible emission under the 366 nm UV light. The paper-strips were consequently dipped into the solutions containing sulfide (of either same or half concentration of that of the probe), and kept them in air for 30 min. The visual fluorescence response of the probe-coated paper strips changed from dark to baby blue under 366 nm UV light in the presence of sulfide (Figure 4b).

With the easy availability and accessibility of smartphones, a new trend of detecting analytes with smartphones has been an emerging area, sometimes popularly termed as “smartphone chemistry”.^{46–49} Since the visual changes of the solution of the probe **1** under the UV light showed distinct differences in the emission intensity, depending on the concentration gradient of sulfide (Figure 4c), we thus explored the possibility of quantification of sulfide in tap water samples using a smartphone Android-based app developed by our group.⁵⁰ The app, initially designed for the color-blind students, can read out the RGB values of an object. Each of the solutions was added to a vial and imaged using a smartphone camera under 366 nm UV light. The smartphone app was then used to decipher the RGB values of the images before and after adding sulfide, and each of the relative ΔR values was obtained by subtracting the average R values of the blank sample (probe **1** only) from those obtained after the addition of sulfide and dividing the resultant by the ‘blank value’. The data were always acquired in relative terms to remove the dependence of the absolute RGB values of probe **1** as the background (blank) value. The concentrations of five blind samples data (containing unknown amounts of sulfide) were estimated and confirmed by the person (not involved in the experiment) who prepared the samples. The relative values of the red channel (extracted from the RGB dataset) were measured and correlated with the known sulfide concentration. From the standard plot (Figure 4d), the blind concentrations of the sulfide samples were successfully determined from the

calibration plot with high accuracy (Table S1, Supporting Information). This enabled the detection of sulfide of environmental samples even by a non-technical person. The method might be proved to be cost-effective⁵¹ and compact for in-field sensing.

Encouraged by the successful *in vitro* application of the probe, efforts were made to detect sulfide in egg chambers of *Drosophila melanogaster*, a standard model for bio-imaging as a part of a live organism (Supporting Information). Adult fruit flies were fattened using dry yeast for 20–24 hours. The ovary was dissected out of adults into 10% fetal bovine serum containing Schneider’s *Drosophila* medium. Dissected ovaries were separated by using micropipette. Two PBS washes were given before incubation with PBS along with probe **1** for 15 min. Egg chambers were further washed with PBS, followed by addition of sulfide and incubation for 30 min. Two PBS washes were given to the samples. Next, they were imaged after mounting in 60% glycerol. The imaging was done with two concentrations of the probe (1 and 0.1 mM) at biological pH upon addition of 4 equiv. (w.r.t. the probe concentration) of sulfide. The imaging was done with two concentrations of the probe **1** i.e. 0.1 mM (Figure 4e) and 1 mM (Figure S15) at biological pH upon addition of sulfide (0.4 and 4 mM respectively). In the presence of sulfide, the fluorescence images of the chambers loaded with probe **1** displayed a bright intracellular luminescence accumulated apparently in the perinuclear regions in contrast to the controls.

The incubation times of 15 min for only probe **1** and 30 min subsequently for sulfide elicited the sufficient fluorometric changes inside the egg chamber. The overall incubation time for probe **1** was deliberately kept small compared to the saturation time (180 min), so as to minimize the effect on the *Drosophila*.

CONCLUSIONS

In conclusion, this work introduces a pair of unconventional detection strategies, namely fusion and fission of annulated rings based on sulfide-induced azide-reduction. We have developed a set of three selective organic probes (appended with ‘active’ or ‘latent’ azido groups) each of which can detect sulfide, following a *de novo* detection mechanism. Two types of detection strategies have been employed in our work: conversion of a pro-fluorophore into another emissive species *via* an *in situ* transformation, and destruction of the ring fused with the fluorophore in order to restore the original emission signature. The mechanisms proposed in this work are established based on well-characterized evidences including crystal structures. One of these easy-to-prepare probes offers practical applications of the detection of sulfide with environmental water as well as in dip-stick analysis. This probe enabled us also for the determination of the blind concentration with RGB analysis using a smartphone and bioimaging in the ovary of fruit-flies.

These novel detection mechanisms may open up a new avenue for further development of this field.

EXPERIMENTAL SECTION

Materials and Instruments. All materials and reagents were commercially available and no further purification was performed unless otherwise noted. Pure solvents were used in dried condition. A dry nitrogen atmosphere was maintained during the reactions using flame-dried glassware, unless otherwise indicated. The structures of the compounds were determined by NMR spectroscopy, mass spectrometry, XRD analysis and a plethora of other spectroscopic techniques. The ^1H NMR spectra were recorded on a 400 MHz JEOL or a 500 MHz Bruker spectrometer instruments. Similarly, ^{13}C NMR experiments were performed with 100 MHz Jeol and 125 MHz Bruker instruments. Chemical shifts reported in this work are values with respect to either an internal reference (TMS) or the solvent peak. The spectroscopy-grade solvents used for the spectroscopic experiments were devoid of any fluorescent impurity. Milli-Q water was used for the spectroscopic experiments. The solutions of anions were prepared from TBAF, TBACl, TBABr, TBAI, TBACN, NaClO_4 , Na_2S , NaN_3 , Na_2SO_4 , NaNO_2 , NaNO_3 , NaSCN , Na_2CO_3 , NaHCO_3 , Na-ascorbate, Na-benzoate, NaBO_3 , Na_2HPO_4 , NaH_2PO_4 , Na_3PO_4 , NaOAc , NaHSO_3 , $\text{Na}_2\text{S}_2\text{O}_3$, $\text{Na}_2\text{S}_2\text{O}_4$, $\text{Na}_2\text{S}_2\text{O}_5$ and K_2S_5 (a polysulfide) in water (TBA = tetrabutylammonium), while the solutions of the neutral molecules were prepared from H_2O_2 , melamine, cysteine and glutathione. IR spectroscopic data were obtained with a Spectrum Two PerkinElmer FT-IR Spectrometer. UV-vis spectra were recorded with a Cary 60 UV-vis spectrophotometer. Fluorescence measurements were carried out with a Horiba Jobin Yvon fluorometer (Fluoromax-4, Xe-150 W, 250–900 nm) and JASCO FP-8300 fluorometer. Optical studies were performed water/DMSO (99:1, v/v), water/MeCN (1:2, v/v) and water/MeCN (2:3, v/v) for probe **1**, **2** and **3**, respectively and all the media were buffered with TRIS (1 mM, at pH 7.4, 25 °C), unless otherwise indicated. Fluorescence imaging experiments were carried out using an Olympus IX 51 inverted microscope with UV excitation and an Axio Observer with Apotome module. HRMS data were obtained from Acquity ultra-performance Bruker MaXis Impact liquid chromatography instrument by positive mode electrospray ionization (Q-TOF). pH data were recorded with a Sartorius Basic Meter PB-11 calibrated at pH 4, 7, and 10. Reactions were monitored by TLC with Merck plates (TLC Silica Gel 60 F254). Silica gel (100–200 mesh, Merck) was used for column chromatographic purification. Yields refer to the chromatographically and spectroscopically pure compounds.

Synthesis.

Experimental Procedures and Spectroscopic characterization of 1, 2, 3, 1a, 2a and 3a. 2-Azidobenzaldehyde was prepared from 2-nitrobenzaldehyde upon treatment

with NaN_3 in HMPA, following the literature procedure.⁵² The other compounds were prepared according to the procedures described below.

Diethyl 2-(2-azidobenzylidene)malonate (1). Piperidine (0.150 mL, 1.52 mmol) was added to the solution of diethylmalonate (0.261 g, 1.63 mmol) in EtOH at 0 °C. After stirring for 10 min, was added dropwise the ethanolic solution of 2-azidobenzaldehyde (0.200 g, 1.36 mmol). After stirring for 4 h at room temperature, the reaction mixture was evaporated to dryness, extracted with DCM (30 mL), and washed with brine (50 mL \times 2). The organic phase was dried over anhydrous Na_2SO_4 and concentrated under reduced pressure. The residue on chromatography with hexane/ethyl acetate (3:1, v/v) yielded compound **1**⁵³ (0.295 g, 75%) as a yellow solid, and recrystallized from DCM/EtOAc mixture. ^1H NMR (400 MHz, CDCl_3): 1.21 (t, J = 6.88 Hz, 3H, CH_3), 1.33 (t, J = 6.88 Hz, 3H, CH_3), 4.26 (q, J = 6.88 Hz, 2H, CH_2), 4.31 (q, J = 6.88 Hz, 2H, CH_2), 7.09 (m, 1H, ArH), 7.19 (m, 1H, ArH), 7.41 (m, 2H, ArH), 7.93 (s, 1H, CH). $^{13}\text{C}\{^1\text{H}\}$ NMR (100 MHz, CDCl_3): 13.7, 14.0, 61.5, 61.6, 118.4, 124.6, 124.9, 127.7, 129.1, 131.4, 137.3, 139.4, 163.8, 166.1. FT-IR (KBr, cm^{-1}): 1697, 1738, 2136. λ_{abs} in water (nm) 250, 286, 335. HRMS (m/z): Calcd. for $\text{C}_{14}\text{H}_{15}\text{N}_3\text{O}_4\text{Na}^+$ or $[\text{M}+\text{Na}]^+$ 312.0965, found 312.0965.

3-(2-azidobenzylidene)pentane-2,4-dione (2). Piperidine (0.150 mL, 1.52 mmol) was added to the solution of acetylacetone (0.136 g, 1.63 mmol) in EtOH at 0 °C. After stirring for 10 min, was added dropwise the ethanolic solution of 2-azidobenzaldehyde (0.200 g, 1.36 mmol). After stirring for 3 h at room temperature, the reaction mixture was evaporated to dryness, extracted with EtOAc (30 mL), and was washed with distilled water (50 mL \times 2), followed by brine (50 mL \times 2). The organic phase was dried over anhydrous Na_2SO_4 and concentrated under reduced pressure. The residue on chromatography with hexane/DCM (4:1, v/v) yielded compound **2**⁵⁴ (0.193 g, 62%) as a light-yellow powder, and recrystallized from DCM/hexane. ^1H NMR (400 MHz, CDCl_3): 2.14 (s, 3H, CH_3), 2.36 (s, 3H, CH_3), 7.03 (t, J = 6.88 Hz, 1H, ArH), 7.14 (d, J = 8.36 Hz, 1H, ArH), 7.22 (d, J = 6.88, 1H, ArH), 7.37 (t, J = 7.64 Hz, 1H, ArH), 7.62 (s, 1H, ArH). $^{13}\text{C}\{^1\text{H}\}$ NMR (100 MHz, CDCl_3): 26.4, 31.6, 118.5, 124.5, 124.3, 129.9, 131.7, 134.7, 139.2, 143.4, 196.5, 204.7. FT-IR (KBr, cm^{-1}): 1650, 1730, 2136. λ_{abs} (nm) in water/MeCN (1:2, v/v) 256, 280, 330. HRMS (m/z): Calcd. for $\text{C}_{12}\text{H}_{11}\text{N}_3\text{O}_2\text{Na}^+$ or $[\text{M}+\text{Na}]^+$ 252.0743, found 252.0735.

Tetrazolo[1,5-a]quinoline-4-carbonitrile (3). A ethanolic solution (5 mL/mmol) of 2-azidobenzaldehyde (0.200 g, 1.36 mmol) was added dropwise to a mixture of malononitrile (0.108 g, 1.63 mmol) and piperidine (0.150 mL, 1.52 mmol) in EtOH at 0 °C. After stirring for 3 h at room temperature, the reaction mixture was evaporated to dryness, extracted with DCM (50 mL), and was washed with distilled water (50 mL \times 2), followed by brine (50 mL \times 2). The organic phase was dried over anhydrous Na_2SO_4 and concentrated under reduced pressure. The residue on

chromatography with hexane/DCM (1:6, v/v) yielded compound **3⁵⁵** (0.181 g, 68%) as yellow powder, and recrystallized from EtOH-DCM. ¹H NMR (500 MHz, DMSO-*d*₆/CD₃CN (4:1; v/v)): 7.92 (t, *J* = 7.65, 1H, ArH), 8.16 (t, *J* = 7.95, 1H, ArH), 8.31 (d, *J* = 7.95 Hz, 1H, ArH), 8.67 (d, *J* = 8.5 Hz, 1H, ArH), 9.16 (s, 1H, ArH). ¹³C{¹H} NMR (125 MHz, DMSO-*d*₆/CD₃CN (4:1; v/v)): 97.2, 113.9, 116.4, 122.6, 128.9, 130.8, 131.4, 134.8, 143.3, 145.7. FT-IR (KBr, cm⁻¹): 1654, 2233, 3066 λ_{abs} (nm) in water/MeCN (2:3, v/v) 290, 298, 330. HRMS (*m/z*): Calcd. for C₁₀H₅N₅Na⁺ or [M+Na]⁺ 218.0437, found 218.0435.

Ethyl 2-oxo-1, 2-dihydroquinoline-3-carboxylate (1a). Sodium sulfide (1.35 g, 17.30 mmol) in water (3 mL) was added dropwise to a solution of compound **1** (1 g, 3.46 mmol) in methanol (50 mL) at 25 °C. After stirring overnight, the reaction was neutralized with 15 mL 0.1 (N) AcOH, extracted with ethyl acetate (25 mL) and washed with distilled water (50 mL×2), and brine (50 mL×2). The organic phase was dried over anhydrous Na₂SO₄ and concentrated under reduced pressure. The residue on chromatography with hexane/ethyl acetate (1:4, v/v) yielded compound **1a** (0.338 g, 60%) as a brown solid. ¹H NMR (400 MHz, CDCl₃): ¹H NMR (400 MHz, CDCl₃): 1.43 (t, *J* = 7.64 Hz, 3H, CH₂CH₃), 4.43 (q, *J* = 7.64 Hz, 2H, CH₂CH₃), 7.23 (t, *J* = 7.64 Hz, 1H, ArH), 7.51-7.63 (m, 3H, ArH), 8.54 (s, 1H, ArH), 12.64 (bs, 1H, NH). ¹³C{¹H} NMR (125 MHz, CDCl₃): 14.2, 61.3, 116.3, 118.5, 122.0, 123.0, 129.1, 133.0, 140.0, 145.6, 161.3, 164.3. FT-IR (KBr, cm⁻¹): 1595, 1647, 1737. λ_{abs} in water (nm) 280, 330. HRMS (*m/z*): Calcd. for C₁₂H₁₁NO₃Na⁺ or [M+Na]⁺ 240.0637, found 240.0623.

1-(2-methylquinolin-3-yl)ethan-1-one (2a). Sodium sulfide (2.55 g, 32.72 mmol) in water (4 mL) was added to a solution of compound **2** (1.5 g, 6.54 mmol) in acetonitrile-dichloromethane (50 mL, 4:1, v/v) at 25 °C. After stirring 4 hr, the reaction was neutralized with 20 mL 0.05 (N) AcOH, extracted with dichloromethane (30 mL) and washed with distilled water (50 mL×2), and brine (50 mL×2). The organic phase was dried over anhydrous Na₂SO₄ and concentrated under reduced pressure. The residue on chromatography with hexane/dichloromethane (1:4, v/v) yielded compound **2a** (0.667 g, 55%) as a solid yellow powder. ¹H NMR (400 MHz, CDCl₃): 2.60 (s, 3H, CH₃), 2.82 (s, 3H, CH₃), 7.44 (t, *J* = 7.64 Hz, 1H, ArH), 7.67 (t, *J* = 8.4 Hz, 1H, ArH), 7.73 (d, *J* = 7.64 Hz, 1H, ArH), 7.95 (d, *J* = 9.16 Hz, 1H, ArH), 8.35 (s, 1H, ArH). ¹³C{¹H} NMR (100 MHz, CDCl₃): 25.2, 28.9, 125.3, 126.4, 128.0, 128.1, 130.7, 131.5, 138.1, 147.7, 157.3, 199.5. FT-IR (KBr, cm⁻¹): 1680. λ_{abs} (nm) in water/MeCN (1:3, v/v) 280. HRMS (*m/z*): Calcd. for C₁₂H₁₂NO⁺ or [M+H]⁺ 186.0913, found 186.0914.

2-aminoquinoline-3-carbonitrile (3a). Compound **3** (1.20 g, 6.14 mmol) was dissolved in dichloromethane (5 mL) and mixed with 50 mL of methanol. Then solution of sodium sulfide (2.40 g, 30.74 mmol) in water (4 mL) was mixed dropwise to the previous mixture at 25 °C. After stirring 6 hr, the solvent of the reaction mixture was removed in

rotary evaporator. The crude solid product was washed with dichloromethane (30 mL) and washed with distilled water (50 mL×2), and brine (50 mL×2). The organic phase was dried over anhydrous Na₂SO₄ and concentrated under reduced pressure. The residue on chromatography with hexane/dichloromethane (1:9, v/v) yielded compound **3a** (0.603 g, 58%) as a solid yellow powder. ¹H NMR (400 MHz, DMSO-*d*₆/D₂O (2:1; v/v)): 2.82 (s, 3H, CH₃), 6.69 (br, 2H, NH₂), 7.28 (t, *J* = 6.88 Hz, 1H, ArH), 7.50 (d, *J* = 8.4 Hz, 1H, ArH), 7.66 (t, *J* = 7.64 Hz, 1H, ArH), 7.74 (d, *J* = 7.64 Hz, 1H, ArH), 8.61 (s, 1H, ArH). ¹H NMR (400 MHz, CDCl₃): 5.36 (br, 2H, NH₂), 7.33 (m, 1H, ArH), 7.66 (m, 3H, ArH), 8.30 (s, 1H, ArH). ¹³C{¹H} NMR (100 MHz, CDCl₃): 95.1, 116.2, 121.8, 124.1, 126.4, 128.1, 133.2, 144.2, 149.1, 154.8. FT-IR (KBr, cm⁻¹): 1654, 2227, 3162, 3321, 3396. λ_{abs} (nm) in water/MeCN (2:3, v/v) 290, 298, 330. HRMS (*m/z*): Calcd. for C₁₀H₈N₃⁺ or [M+H]⁺ 170.0713, found 170.0712.

ASSOCIATED CONTENT

Supporting Information

Spectroscopic and spectrometric characterization of the compounds, fluorescence detection, single crystal X-ray diffraction data, and computational analysis.

Crystal data of compound **1** (CCDC 1879384)

Crystal data of compound **1a** (CCDC 1879400)

Crystal data of compound **2** (CCDC 1912153)

Crystal data of compound **2a** (CCDC 1912155)

Crystal data of compound **3** (CCDC 1912156)

Crystal data of compound **3a** (CCDC 1912158)

AUTHOR INFORMATION

Corresponding Author

*E-mail: sb1@iiserkol.ac.in.

Subhajit Bandyopadhyay: 0000-0001-7668-0274

Present Addresses

†If an author's address is different than the one given in the affiliation line, this information may be included here.

Author Contributions

The manuscript was written through contributions of all authors. All authors have given approval to the final version of the manuscript.

Notes

The authors declare no competing financial interest.

ACKNOWLEDGMENT

This work is funded by a Ministry of Human Resources grant for Swachhata (Clean India) Action Plan (ICSR/SAP/2018/SN-1) to S.B. B.R. and S.G. are supported by INSPIRE and CSIR fellowship respectively. The help of Mr. Sayanur Rahaman, Mr. Sudipta Halder and Dr. Sudipta Bar for the biological and imaging experiments is greatly appreciated. Mr. Supriya Sasmal is gratefully acknowledged for

crystallography and Ms. Tiasha Saha Roy for her help with data analysis.

REFERENCES

- Papapetropoulos, A.; Pyriochou, A.; Altaany, Z.; Yang, G.; Marazioti, A.; Zhou, Z.; Jeschke, M. G.; Branski, L. K.; Herndon, D. N.; Wang, R.; Szabó, C. Hydrogen Sulfide is an Endogenous Stimulator of Angiogenesis. *Proc. Natl. Acad. Sci. U.S.A.* **2009**, *106*, 21972–21977.
- Yang, G.; Wu, L.; Jiang, B.; Yang, W.; Qi, J.; Cao, K.; Meng, Q.; Mustafa, A. K.; Mu, W.; Zhang, S.; Snyder, S. H.; Wang, R. H₂S as a Physiologic Vasorelaxant: Hypertension in Mice with Deletion of Cystathionine γ -Lyase. *Science* **2008**, *322*, 587–590.
- Prabhakar, N. R. Sensing Hypoxia: Physiology, Genetics and Epigenetics. *J. Physiol.* **2013**, *591*, 2245–2257.
- Li, Q.; Sun, B.; Wang, X.; Jin, Z.; Zhou, Y.; Dong, L.; Jiang, L.-H.; Rong, W. A Crucial Role for Hydrogen Sulfide in Oxygen Sensing via Modulating Large Conductance Calcium-Activated Potassium Channels. *Antioxid. Redox Signal.* **2009**, *12*, 1179–1189.
- <https://www.osha.gov/SLTC/hydrogensulfide/hazards.html> (last accessed April 24, 2019).
- Hydrogen Sulfide; World Health Organization: Geneva, 1981.
- Gosselin, R. E.; Smith, R. P.; Hodge, H. C. Hydrogen Sulfide. In *Clinical Toxicology of Commercial Products*, 5th ed.; Williams and Wilkins: Baltimore, MD, 1984; pp III-198–202.
- Knight, L. D.; Presnell, S. E. Death by Sewer Gas: Case Report of a Double Fatality and Review of the Literature. *Am. J. Forensic Med. Pathol.* **2005**, *26*, 181–185.
- Guidotti, T. L. Hydrogen Sulfide: Advances in Understanding Human Toxicity. *Int. J. Toxicol.* **2010**, *29*, 569–581.
- <http://publichealth.lacounty.gov/acd/reports/splrpts/spcrpt05/DeathsHydrogenSulfide05.pdf> (last accessed April 24, 2019).
- <https://www.latimes.com/archives/la-xpm-2005-sep-03-me-port3-story.html> (last accessed July 17, 2019).
- Szinicz, L. History of Chemical and Biological Warfare Agents. *Toxicol.* **2005**, *214*, 167–181.
- Croddy, E.; Perez-Armendariz, C.; Hart, J. *Chemical and Bio-logical Warfare: A Comprehensive Survey for the Concerned Citizen*, Springer, New York, 2001.
- Virji, S.; Fowler, J. D.; Baker, C. O.; Huang, J.; Kaner, R. B.; Weiller, B. H. Polyaniline Nanofiber Composites with Metal Salts: Chemical Sensors for Hydrogen Sulfide. *Small* **2005**, *1*, 624–627.
- <https://edition.cnn.com/2017/08/03/asia/australia-plane-terror-plot-isis/index.html> (last accessed July 17, 2019).
- MacDonald, R. S.; Wagner, K. Influence of Dietary Phytochemicals and Microbiota on Colon Cancer Risk. *J. Agric. Food Chem.* **2012**, *60*, 6728–6735.
- Qu, K.; Lee, S. W.; Bian, J. S.; Low, C. M.; Wong, P. T. H. Hydrogen Sulfide: Neurochem-
- istry and Neurobiology. *Neurochem. Int.* **2008**, *52*, 155–165.
- Kamoun, P.; Belardinelli, M. -C.; Chabli, A.; Lallouchi, K.; Chadefaux-Vekemans, B. Endogenous Hydrogen Sulfide Overproduction in Down Syndrome. *Am. J. Med. Genet. A* **2013**, *116*, 310–311.
- Yang, W.; Yang, G.; Jia, X.; Wu, L.; Wang, R. Activation of K_{ATP} Channels by H₂S in Rat Insulin-Secreting Cells and the Underlying Mechanisms. *J. Physiol.* **2005**, *569*, 519–531.
- Fiorucci, S.; Antonelli, E.; Mencarelli, A.; Orlandi, S.; Renga, B.; Rizzo, G.; Distrutti, E.; Shah, V.; Morelli, A. The Third Gas: H₂S Regulates Perfusion Pressure in both the Isolated and Perfused Normal Rat Liver and in Cirrhosis. *Hepatology* **2005**, *42*, 539–548.
- <https://ohsonline.com/articles/2007/10/human-health-effects-from-exposure-to-lowlevel-concentrations-of-hydrogen-sulfide.aspx> (last accessed July 17, 2019).
- Jiang, J.; Chan, A.; Ali, S.; Saha, A.; Haushalter, K. J.; M. Lam, W.-L.; Glasheen, M.; Parker, J.; Brenner, M.; Mahon, S. B.; Patel, H. H.; Ambudhan, R.; Lipton, S. A.; Pilz, R. B.; Boss, G. R. Hydrogen Sulfide—Mechanisms of Toxicity and Development of an Antidote. *Sci. Rep.* **2016**, *6*, 20831.
- For excellent reviews: Yang, Y.; Zhao, Q.; Feng, W.; Li, F. Luminescent Chemodosimeters for Bioimaging. *Chem. Rev.* **2013**, *113*, 192–270.
- Ashton, T. D.; Jolliffe, K. A.; Pfeffer, F. M. Luminescent Probes for the Bioimaging of Small Anionic Species in vitro and in vivo. *Chem. Soc. Rev.* **2015**, *44*, 4547–4595.
- Liu, C.; Peng, B.; Li, S.; Park, C.-M.; Whorton, A. R.; Xian, M. Reaction Based Fluorescent Probes for Hydrogen Sulfide. *Org. Lett.* **2012**, *14*, 2184–2187.
- Jiao, X.; Li, Y.; Niu, J.; Xie, X.; Wang, X.; Tang, B. Small-Molecule Fluorescent Probes for Imaging and Detection of Reactive Oxygen, Nitrogen, and Sulfur Species in Biological Systems. *Anal. Chem.* **2018**, *90*, 533–555.
- Zheng, H.; Zhan, X.-Q.; Bian, Q.-N.; Zhang, X.-J. Advances in Modifying Fluorescein and Rhodamine Fluorophores as Fluorescent Chemosensors. *Chem. Commun.* **2013**, *49*, 429–447.
- Li, J.; Yin, C.; Huo, F. Chromogenic and Fluorogenic Chemosensors for Hydrogen Sulfide: Review of Detection Mechanisms since the Year 2009. *RSC Adv.* **2015**, *5*, 2191–2206.
- Guo, Z.; Chen, G.; Zeng, G.; Li, Z.; Chen, A.; Wang, J.; Jiang, L. Fluorescence Chemosensors for Hydrogen Sulfide Detection in Biological Systems. *Analyst* **2015**, *140*, 1772–1786.
- Peng, H.; Cheng, Y.; Dai, C.; King, A. L.; Predmore, B. L.; Lefer, D. J.; Wang, B. A Fluorescent Probe for Fast and Quantitative Detection of Hydrogen Sulfide in Blood. *Angew. Chem. Int. Ed.* **2011**, *50*, 9672–9675.
- Chen, S.; Chen, Z.; Ren, W.; Ai, H. Reaction-Based Genetically Encoded Fluorescent Hydrogen Sulfide Sensors. *J. Am. Chem. Soc.* **2012**, *134*, 9589–9592.
- Lin, V. S.; Lippert, A. R.; Chang, C. Cell-Trappable Fluorescent Probes for Endogenous Hydrogen Sulfide Signaling and Imaging H₂O₂-

- Dependent H₂S Production. *J. Proc. Natl. Acad. Sci. U.S.A.* **2013**, *110*, 7131–7135.
33. Zhang, J.; Guo, W. A New Fluorescent Probe for Gasotransmitter H₂S: High Sensitivity, Excellent Selectivity, and a Significant Fluorescence Off-On Response. *Chem. Commun.* **2014**, *50*, 4214–4217.
34. Tang, Y.; Xu, A.; Ma, Y.; Xu, G.; Gao, S.; Lin, W. A Turn-On Endoplasmic Reticulum-Targeted Two-Photon Fluorescent Probe for Hydrogen Sulfide and Bio-Imaging Applications in Living Cells, Tissues, and Zebrafish. *Sci. Rep.* **2017**, *7*, 12944.
35. Nagarkar, S. S.; Saha, T.; Desai, A. V.; Talukdar, P.; Ghosh, S. K. Metal-Organic Framework Based Highly Selective Fluorescence Turn-On Probe for Hydrogen Sulphide. *Sci. Rep.* **2014**, *4*, 7053.
36. Wu, Z.; Li, Z.; Yang, L.; Han, J.; Han, S. Fluorogenic Detection of Hydrogen Sulfide via Reductive Unmasking of O-Azidomethylbenzoyl-Coumarin Conjugate. *Chem. Commun.* **2012**, *48*, 10120–10122.
37. Bae, S. K.; Heo, C. H.; Choi, D. I.; Sen, D.; Joe, E.-H.; Cho, B. R.; Kim, H. M. A Ratiometric Two-Photon Fluorescent Probe Reveals Reduction in Mitochondrial H₂S Production in Parkinson's Disease Gene Knockout Astrocytes. *J. Am. Chem. Soc.* **2013**, *135*, 9915–9923.
38. Liu, X.-L.; Du, X.-J.; Dai, C.-G.; Song, Q.-H. Ratiometric Two-Photon Fluorescent Probes for Mitochondrial Hydrogen Sulfide in Living Cells. *J. Org. Chem.* **2014**, *79*, 9481–9489.
39. Cao, J.; Lopez, R.; Thacker, J. M.; Moon, J. Y.; Jiang, C.; Morris, S. N. S.; Bauer, J. H.; Tao, P.; Mason, R. P.; Lippert, A. R. Chemiluminescent Probes for Imaging H₂S in Living Animals. *Chem. Sci.* **2015**, *6*, 1979–1985.
40. Kim, M.; Hun Seo, Y.; Kim, Y.; Heo, J.; Jang, W.-D.; Jun Sim, S.; Kim, S. A Fluorogenic Molecular Nanoprobe with an Engineered Internal Environment for Sensitive and Selective Detection of Biological Hydrogen Sulfide. *Chem. Commun.* **2017**, *53*, 2275–2278.
41. Lippert, A. R.; New, E. J.; Chang, C. J. Reaction-Based Fluorescent Probes for Selective Imaging of Hydrogen Sulfide in Living Cells. *J. Am. Chem. Soc.* **2011**, *133*, 10078–10080.
42. Owing to the controversies on the actual form of sulfide that exists in aqueous solution, we shall simply refer the species as 'sulfide'. For further details: May, P. M.; Batka, D.; Hefter, G.; Königsberger, E.; Rowland, D. Goodbye to S²⁻ in Aqueous Solution. *Chem. Commun.* **2018**, *54*, 1980–1983.
43. World Health Organization. (1996). Guidelines for drinking-water quality. Vol. 2, Health criteria and other supporting information.
44. Henthorn, H. A.; Pluth, M. D. Mechanistic Insights into the H₂S-Mediated Reduction of Aryl Azides Commonly Used in H₂S Detection. *J. Am. Chem. Soc.* **2015**, *137*, 15330–15336.
45. Li, W.; Sun, W.; Yu, X.; Du, L.; Li, M. Coumarin-Based Fluorescent Probes for H₂S Detection. *J. Fluoresc.* **2013**, *23*, 181–186.
46. McCracken, K. E.; Yoon, J. Y. Recent Approaches for Optical Smartphone Sensing in Resource-Limited Settings: a Brief Review. *Anal. Methods* **2016**, *8*, 6591–6601.
47. Cherbuin, M.; Zelder, F.; Karlen, W. Quantifying Cyanide in Water and Foodstuff Using Corrin-Based Cyanokit Technologies and a Smartphone. *Analyst* **2019**, *144*, 130–136.
48. Roy, B.; Roy, T. S.; Rahaman, S. A.; Das, K.; Bandyopadhyay, S. A Minimalist Approach for Distinguishing Individual Lanthanide Ions Using Multivariate Pattern Analysis. *ACS Sens.* **2018**, *3*, 2166–2174.
49. Ji, X.; Chen, W.; Long, L.; Huang, F.; Sessler, J. L. Double Layer 3D Codes: Fluorescent Supramolecular Polymeric Gels Allowing Direct Recognition of the Chloride Anion Using a Smart Phone. *Chem. Sci.* **2018**, *9*, 7746–7752.
50. Bandyopadhyay, S.; Rathod, B. B. The Sound and Feel of Titrations: a Smartphone Aid for Color-Blind and Visually Impaired Students. *J. Chem. Educ.* **2017**, *94*, 946–949.
51. Wilson, D. J.; Kumar, A. A.; Mace, C. R. Overreliance on Cost Reduction as a Featured Element of Sensor Design. *ACS Sens.* **2019** (DOI: 10.1021/acssensors.9b00260).
52. Guggenheim, K. G.; Toru, H.; Kurth, M. J. One-pot, two-step cascade synthesis of quinazolinotriazolobenzodiazepines. *Org. Lett.* **2012**, *14*, 3732–3735.
53. Chaabouni, S.; Pinkerton, N. M.; Abid, S.; Gallaup, C.; Chassaing, S. Photochemistry of ortho-Azidocinnamoyl Derivatives: Facile and Modular Synthesis of 2-Acylated Indoles and 2-Substituted Quinolines under Solvent Control. *Synlett* **2017**, *28*, 2614–2618.
54. Zhao, F. F.; Yan, Y. M.; Zhang, R.; Ding, M. W. Efficient one-pot synthesis of 1H-pyrazolo [1, 5-b] indazoles by a domino Staudinger-aza-Wittig cyclization. *Synlett* **2012**, *23*, 2850–2852.
55. Shivakumar, K.; Vidyasagar, A.; Naidu, A.; Gonnade, R. G.; Sureshan, K. M. Strength from weakness: The role of CH... N hydrogen bond in the formation of wave-like topology in crystals of aza-heterocycles. *CrystEngComm* **2012**, *14*, 519–524.

1
2
3
4
5
6
7
8
9
10
11
12
13
14
15
16
17
18
19
20
21
22
23
24
25
26
27
28
29
30
31
32
33
34
35
36
37
38
39
40
41
42
43
44
45
46
47
48
49
50
51
52
53
54
55
56
57
58
59
60

Formation or cleavage of rings *via* sulfide-mediated reduction offers background-free detection of sulfide

